

Adaptive Routing using Relative Cost Concept in Elastic Optical Networks with Space-Division Multiplexing

Anwar Alyatama^{1,*}  and Mona Ali¹

¹Computer Engineering Department, Kuwait University, Sabah Al Salem University City 74252, Kuwait

*Corresponding author: Anwar Alyatama, a.yatama@ku.edu.kw

Article Information

Article History:

Received: 5 December 2023

Revised: 1 January 2024

Accepted: 3 April 2024

Published: 19 October 2025

Keywords:

Elastic Optical Networks

Relative Cost

Routing and Resource Allocation

Space Division Multiplexing

Abstract

Elastic Optical Networks with Space Division Multiplexing Networks (EON-SDM) is the most prominent technology for efficiently transmitting massive amounts of data flow and dealing with the explosion of new technologies that require a wide range of services. Among the various factors that determine network efficiency, performance, and design effectiveness in EON-SDM networks is routing, spectrum, and core allocation (RSCA). RSCA's strategic optimization ensures efficient data transmission, effortlessly meeting the demands of high-bandwidth applications. Within this study, we propose a relative cost-based adaptive RSCA algorithm that prioritizes long-term state consequences in accepting new calls. When a call is received, the proposed approach picks the route, core, and spectrum group with the lowest relative cost and compares it to the call's value, in the event that the minimum computed relative cost of the arrival call is greater than the call value, the call is blocked. Comparative analysis with established routing methods reveals promising performance outcomes, including a 45% reduction in normalized loss revenue and a 155% enhancement in fairness in certain scenarios.

1. Introduction

The rapid growth of internet traffic in recent years, driven by data-centric and automated systems, underscores the imminent requirement for a specific type of network infrastructure. Such a network would facilitate the swift and seamless transmission of massive volumes of data. A significant potential is seen in the Elastic Optical Network with Space Division Multiplexing (EON-SDM) as a technology solution for efficiently transmitting massive amounts of data flow and navigating the emergence of new technologies. Through the substantial increase in spectral resources, EON-SDM introduces a new dimension: the spatial dimension. Multi-core fibers (MCF), for instance, allow each fiber to have many cores, each supporting the transmission of a single mode. In contrast, few-mode fibers (FMF) have a single, large core in each fiber, enabling the transmission of various modes.

With the introduction of the spatial dimension in SDM networks, routing, core, and spectrum allocation, or RSCA, now forms part of the resource allocation problem. Numerous strategies and methods have been

proposed to solve the RSCA problem (Da S. Oliveira and Da Fonseca, 2022; Heera et al., 2023; Lan et al., 2022; Petale and Subramaniam, 2023; Sharma et al., 2022; Seki et al., 2022; Vasundhara et al., 2023). Their methods for choosing a route, a core, and a starting frequency slot are different, as are their underlying presumptions. The following pivotal assumptions are made: whether incoming traffic is known ahead of time, whether the modulation format is static or adaptive, whether MCF crosstalk between cores is computed, whether core switching is implemented. Additionally, we consider whether the RSCA problem is uncoupled into subproblems.

This work centers on the online RSCA problem for MCF without inter-core crosstalk. In this specific context, the performance metric hinges on the percentage of calls that get blocked due to resource limitations. Accurately estimating call blocking probabilities at specific traffic demands becomes crucial. Network planners leverage these predictions to design networks that deliver the bare minimum acceptable service to users.

The introduced algorithm builds upon our earlier contributions outlined in references (Alyatama, 2017)

and (Alyatama, 2020b). In (Alyatama, 2017), the relative cost technique was initially investigated and determined to be viable method for resolving online resource sharing problems. The work in Alyatama (2020b) developed an adaptable routing, and spectrum allocation RSA method that compute the relative cost of admitting a newly arrived call for all available routes and starting frequency slots. This call is carried on the route and starting frequency slot with the minimum computed relative cost however, the call is rejected if no resource is available that matches the request requirements, or if the smallest computed relative cost is greater than the call value. Therefore, agreeing to a call with a lower reward decreases the chances of obtaining a higher reward, resulting in the rejection of certain lower-reward calls to accommodate higher-paying ones. Alyatama (2020a) proposed an adaptive multi-path routing and spectrum allocation (RSA) method based on the relative cost approach. Additionally, the research discussed in Alyatama (2021b) expands on the adaptive RSA algorithm, which is grounded in relative cost considerations, to address the routing, modulation level, and spectrum assignment (RMSA) within elastic optical networks (EON).

This paper presents an adaptive RSCA algorithm for EON-SDM networks with MCF fibers, leveraging the concept of relative cost. For each incoming call, the relative cost is computed for each core, route, and set of available spectrum blocks. Echoing the principles of software-defined networks, a centralized controller with a comprehensive and real-time understanding of network resource allocation serves as the cornerstone for this proposal. The call will be accepted based on the core, route, and set of spectrum blocks with the lowest relative cost. If the minimum relative cost value of the incoming call is higher than its own value, the call will be blocked to accommodate more profitable future calls. The algorithm assumes no crosstalk between nearby cores, allowing calls to be allocated in the same frequency slots.

The following sections are structured as follows. Section 2 commences with an introduction to the network model, the approach for measuring network performance, and the formula for calculating single-link parameters. Following that, in Section 3, we offer context and justification for integrating the relative cost principle. Section 4 provides a detailed explanation of the proposed adaptive RCSA algorithm, supplemented with several illustrative examples (Section 5). Finally, we present our numerical findings in Section 6 and summarize our conclusions in Section 7.

2. Network Model

We assume an Elastic Optical network with Spatial Division Multiplexing (SDM). Links are assumed to be Multi-core links with total number of cores in each link

is C . The available core bandwidth is subdivided into standardized frequency slots of fixed bandwidth, such as 25, 12.5, or even 6.25 GHz. Each of these frequency slots is denoted as f_s . Hereafter, the notation f_s shall be used to refer to each frequency slot, and the total number of slots available on a core is represented by F . Consequently, each core is equipped with a bandwidth allocation of F slots, numbered sequentially from 1 (associated with the minimum frequency) to F (associated with the maximum frequency).

Various call categories (denoted by I) have distinct bandwidth needs, with each type- i requiring a set of t_i contiguous f_s 's, represented as $T = (t_1, t_2, \dots, t_I)$. For the sake of simplicity, we assume that $t_i < t_{i+1}$. Upon a type- i call arrival, the network controller aims to locate t_i contiguous and consecutive frequency slots f_s that are simultaneously available on every link along a specific route from the source to the destination. In simpler terms, the source aims to find an unoccupied set of t_i consecutive frequency slots on route r , starting from frequency slot $f \in F$. If core switching is not implemented, this set of contiguous and consecutive frequency slots f_s must be available on the same core $c \in C$ for all links in route r . Conversely, core switching enhances network flexibility and eliminates the necessity for a continuous core. Type- i calls arrive according to a Poisson process with rate λ_i , while their service times follow a general distribution (see Lea and Alyatama (1995)). The following additional definitions and notations are used:

- N represents the total number of nodes in the network.
- E indicates the total number of edges in the network.
- w_i represents the revenue earned from accepting a call of type $i \in I$.
- B_i stands for the blocking probability for call type i . We can reasonably assume that $w_i = t_i$, meaning the demand value is equal to the demand capacity.
- $\pi_\epsilon(\tau)$ provides a snapshot of the available resources on link ϵ at a specific time τ . For convenience, we use the shorthand notation π_ϵ to represent this state.
- $\pi_{\epsilon-t_i@f,c_\epsilon}$ represents the modified state of link ϵ , where t_i contiguous frequency slots, beginning at frequency f within core c_ϵ , are temporarily reserved.
- $R_{\epsilon,t_i,f,c_\epsilon}$ represents the relative cost associated with admitting a request that requires t_i contiguous frequency slots on link ϵ , commencing from frequency slot f in core c_ϵ .
- $\vec{R}_{r,t_i,f,\bar{c}}$ stands for the relative cost of accepting a request that demands t_i contiguous frequency

slots on route r , starting from frequency slot f in core vector \vec{c} . Without core switching, every link on route r is constrained to operate on the same core.

Finally, core classification technique maybe deployed to mitigate fragmentation in EOS-SDM (Hayashi et al., 2011). Under this approach, cores are classified based on the received demand size t_i . Each core is designated to manage a specific category of demand, guaranteeing that demands requiring the same number of frequency slots are directed to their respective cores. As a result, when a particular demand is satisfied and leaves the system, it opens up capacity for future requests of the same category. However, there are instances when certain cores are tasked with accommodating all types of demands. In such cases, this approach leads to a decreased likelihood of blocking, especially when all the dedicated cores are fully allocated.

2.1 Network Performance Metrics

The network performance is assessed based on the total revenue loss (in \$) caused by rejected calls (Alyatama, 2021b). The network's total revenue loss, denoted by L , is calculated by summing the product of the blocking probability (B_i), request value (w_i), and arrival rate (λ_i) for each call type i within the set I , i.e.,

$$L = \sum_{i=1}^I w_i \lambda_i B_i \text{ $.} \quad (1)$$

The total revenue V is defined as

$$V = \sum_{i=1}^I w_i \lambda_i \text{ $,} \quad (2)$$

and the normalized lost revenue is $N = L/V$. The network's overall blocking probability (G), also known as the network grade-of-service, signifies the average end-to-end blocking probability across all call types.

$$G = \frac{1}{I} \cdot \sum_{i=1}^I B_i. \quad (3)$$

The network grade-of-service G varies between 0.1% for light load and 10% for heavy load (Dlamini, 2023). Elastic optical networks exhibit a significant disparity in fairness for calls with higher bandwidth requirements or longer routes. Therefore, we employ the fairness index used in (Alyatama, 2014) to evaluate the fair allocation of network resources to incoming demands, which is defined as follows:

$$\text{Fairness Index} = \frac{\left(\sum_{i=1}^I B_i\right)^2}{I \cdot \sum_{i=1}^I B_i^2}. \quad (4)$$

The objective is to ensure that every call has a similar chance of being blocked, regardless of its type or

length. This translates to minimizing the variation in their route blocking probabilities, aiming for a fairness index close to 1 (perfect fairness). While traditional algorithms employ resource-based admission control, our proposed algorithm leverages a fairness-aware approach. This enables prioritizing high-demand calls, even with available resources, to optimize long-term resource allocation and achieve greater balance within the system.

2.2 EON-SDM Single Link Blocking Probabilities

To provide a comprehensive understanding, we outline the approach described in (Alyatama, 2021a) that is utilized to calculate the probabilities of single-link blocking in an EON-SDM. The method relies on the concept of superposition, by individually considering each type of traffic before layering all the results on each other (Alyatama, 2016). The calculation accounts for the process of core selection, where calls that are rejected in one core are subsequently directed to the next core in a sequential manner. Moreover, for each individual call type i , each core is divided into F/t_i stages and each stage has a size of t_i and does not share any spectrum overlap with adjacent stages. If the traffic presented to a stage is declined, it will endeavor to utilize the subsequent stage until the call is either accepted or blocked. Each stage analyzes and evaluates three distinct traffic patterns: (1) overflow type- i traffic from the preceding stage, (2) internal background traffic generated by smaller calls utilizing only a portion of the stage's resources, and (3) external background traffic arising from calls requiring the full capacity of the stage. The calculation of blocking probabilities entails an iterative process. Shown in Figure 6 is an illustration of traffic with four types in a single link, where $F = 32f_s$. The figure demonstrates 32 stages for a call demanding 1 frequency slot, 16 stages for a call requiring 2 frequency slots, eight stages for a call necessitating 4 frequency slots, and four stages for a call mandating 8 frequency slots.

In conclusion, the single-link blocking probabilities are used to compute the loss revenue $l(\pi_\epsilon)$ when a call of type i arrives, and $l(\pi_{\epsilon-t_i @ f, c_\epsilon})$ when a call is accepted at starting frequency f on core c_ϵ . For each starting frequency f on core c_ϵ , the relative cost is defined as

$$R_{(\epsilon, t_i, f, c_\epsilon)} = l(\pi_{\epsilon-t_i @ f, c_\epsilon}) - l(\pi_\epsilon).$$

The key parameter required for the single-link computation is the estimated arrival rate of calls of type i on link ϵ . It is assumed that the network central controller can monitor the number of type- i calls currently being transmitted over link ϵ . The average traffic carried on link ϵ can then be estimated using a moving average approach.

The reduced-load model is employed to estimate the type- i arrival rate on link ϵ . Under this model, the offered type- i traffic for link ϵ is assumed to be equivalent

0	1	2	3	4	5	6	7	8	9	10	11	12	13	14	15	16	17	18	19	20	21	22	23	24	25	26	27	28	29	30	31				
$i=4, S=0$																																			
$i=3, S=0$								$i=4, S=1$								$i=3, S=2$								$i=4, S=2$								$i=4, S=3$			
$i=2, S=0$	$i=2, S=1$	$i=2, S=2$	$i=2, S=3$	$i=2, S=4$	$i=2, S=5$	$i=2, S=6$	$i=2, S=7$	$i=2, S=8$	$i=2, S=9$	$i=2, S=10$	$i=2, S=11$	$i=2, S=12$	$i=2, S=13$	$i=2, S=14$	$i=2, S=15$	$i=2, S=16$	$i=2, S=17$	$i=2, S=18$	$i=2, S=19$	$i=2, S=20$	$i=2, S=21$	$i=2, S=22$	$i=2, S=23$	$i=2, S=24$	$i=2, S=25$	$i=2, S=26$	$i=2, S=27$	$i=2, S=28$	$i=2, S=29$	$i=2, S=30$	$i=2, S=31$				
$S=0$	$S=1$	$S=2$	$S=3$	$S=4$	$S=5$	$S=6$	$S=7$	$S=8$	$S=9$	$S=10$	$S=11$	$S=12$	$S=13$	$S=14$	$S=15$	$S=16$	$S=17$	$S=18$	$S=19$	$S=20$	$S=21$	$S=22$	$S=23$	$S=24$	$S=25$	$S=26$	$S=27$	$S=28$	$S=29$	$S=30$	$S=31$				

Figure 1. Illustrating an instance of traffic with four types $I = 4$ and using frequency slots $T = 1, 2, 4, 8$ in a single link with a total of $32f_s$. The frequency slots for the link are numbered from 0 (lowest frequency) to 31 (highest frequency). The link is divided into $32/t_i$ stages for each call type i , where each stage has a size of t_i , and there is no spectrum overlap between the stages. The illustration shows 32 stages of type 1 traffic ($t_1 = 1f_s$), 16 stages of type 2 traffic ($t_2 = 2f_s$), eight stages of type 3 traffic ($t_3 = 4f_s$), and four stages of type 4 traffic ($t_4 = 8f_s$). Blocking probability is computed in consecutive stages, with each stage assessing three types of traffic flows (overflow, internal and external background traffic).

to the carried type- i traffic for link e , under the condition that link e is available for type- i traffic. For further details, readers are encouraged to consult the cited references.

3. Overview of Relative Cost Concept

The link relative cost acts as a measurement to evaluate the cost of carrying a call on a particular set of contiguous frequency slots within a specific core. The calculation of link relative cost involves determining the difference in potential revenue loss before and after the call is accepted. Specifically, when a call i arrives on link e during state π_e , the anticipated future loss is represented as $l(\pi_e)$ \$. When the call is transmitted via link e using the initial frequency slot f and core c , the link transitions to state $\pi_{e-t_i} @ f, c_e$, which possesses a reduced number of available contiguous frequency slots. As a result, the projected future loss becomes $l(\pi_{e-t_i} @ f, c_e)$ \$, leading to the establishment of the relative cost denoted as $R_{e,t_i,f,c_e} = l(\pi_{e-t_i} @ f, c_e) - l(\pi_e)$ \$.

To illustrate the feasibility of using relative cost, consider a simplified scenario that consists of a single link, a single core, and four traffic types $I = 4$, and $T = 1, 2, 4, 8$ characterized by uniform moderate demand. Figure 2 illustrates the impact of link capacity F on lost revenue $l(\pi_e)$. More precisely, a one-unit decrease in link capacity, transitioning from 8 to 7 units of capacity, increases the loss of link revenue noticeably, increasing from 1.44 to \$2.5. Thus, a call with a requirement of $t_4 = 8f_s$, would consistently encounter rejection if the link is restricted to $F = 7$ or less. Similarly, the network performance degrades less noticeably when capacity decreases from 16 to 15, from 24 to 23, and from 4 to 3. Hence, a granted request that utilizes just a single f_s is capable of inflicting a greater impact on the revenue compared to the call valued at ($w_1 = \$1$) when the number of available free capacities are 8, 16, 24, or even 32. For a more in-depth exploration, readers are directed to reference.

4. Proposed RSCA

As previously stated, in order to accommodate a call needing t_i frequency slots, the process involves seeking a route r that commences with a specific frequency slot f_s on core c and is able to utilize t_i contiguous frequency slots, alongside the guard bands. The RSCA algorithm, as presented, presupposes that the network's state is refreshed with the arrival of a new call. Subsequently, it computes the relative cost $\vec{R}_{r,t_i,f,\vec{c}}$ for all accessible continuous and contiguous frequency slots across all routes. The RSCA algorithm opts for the route r , starting frequency index f , and core vector \vec{c} that minimizes the relative cost $\vec{R}_{r,t_i,f,\vec{c}}$. The relative cost of the route is determined by summing the relative costs of all links within that route, represented as:

$$\vec{R}_{r,t_i,f,\vec{c}} = \sum_{e \in r} R_{e,t_i,f,c_e} \$ \quad (5)$$

However, if the minimum relative cost $\vec{R}_{r,t_i,f,\vec{c}}$ multiplied by the discount factor γ exceeds the call's value, then the call is accordingly blocked. Thus, even with resources available, a call may be rejected to ensure future calls with higher resource needs are accommodated.

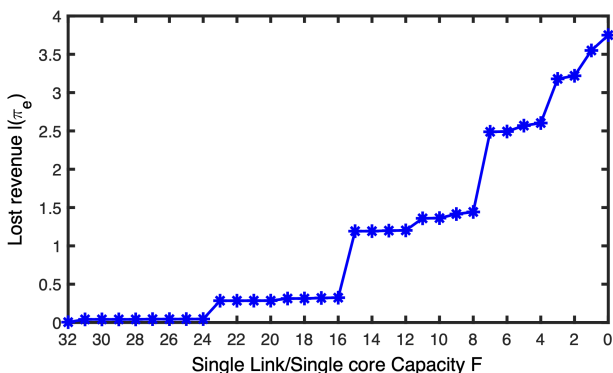


Figure 2. A single link, a single core, and four traffic types. The set of required frequency slots for these traffic types is $T = 1, 2, 4, 8$. The x-axis represents the available link capacity, designated as F , ranging from 32 to 0 frequency slots. The y-axis displays the amount of revenue lost due to calls being blocked, denoted as $l(\pi_e)$.

Here, γ represents the discount rate, signifying the prioritization of present costs over future ones. As a result, the relative cost is adjusted by assuming that a cost incurred in the next period is equivalent to γ times its value in the current period (where $0 < \gamma < 1$).

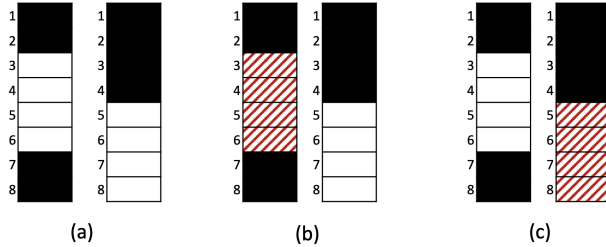


Figure 3. A single link, denoted as e , with two cores $C = 2$ and a total of $F = 8$ frequency slots per core. (a) The link is currently in state π_e where some frequency slots are occupied (colored black) and others are available (colored white). To determine the lost link revenue, $l(e)$, for this state π_e , only the idle frequency slots are considered, while the occupied frequency slots are skipped. For a call demanding four contiguous frequency slots, there are two potential options. (b) Option one accepting the call at starting frequency slot $f = 3$ on the first core $c = 1$ (colored red) or (c) Option two accepting the call at starting frequency slot $f = 5$ on the second core $c = 2$ (colored red).

5. Illustrative Example

5.1 Single Link Core and Spectrum Allocation

We consider a SDM link e with two cores $C=2$ and each core has $F = 8f_s$ i.e., total link capacity is $16f_s$. The link supports three distinct types of calls $I = 3$. Upon arrival at link e , a type 3 call, which requires four frequency slots $t_3 = 4$, encounters the link at state π_e , as illustrated in Figure 3a. First, the lost link revenue $l(e)$ for this state π_e is calculated as described in section 2.2. Two options exist for accepting the newly arrived call, as illustrated in Figures 3b and 3c. Thus, we need to calculate $l(\pi_{e-4@3,1})$ if the call is accepted at starting frequency slot $f = 3$ on the first core $c = 1$ and $l(\pi_{e-4@5,2})$ if the call is accepted at starting frequency slot $f = 5$ on the second core $c = 2$. Finally, the relative cost for the first option is $R_{e,4,3,1} = l(\pi_{e-4@3,1}) - l(e)$ whereas the relative cost for the second option is $R_{e,4,5,2} = l(\pi_{e-4@5,2}) - l(e)$.

5.2 Routing, Core and Spectrum Allocation

Figure 4 depicts a portion of a network with two routes connecting source A to destination D as follows:

- Route 1 consists of link 1 and link 2.

- Route 2 consists of link 3 and link 4.

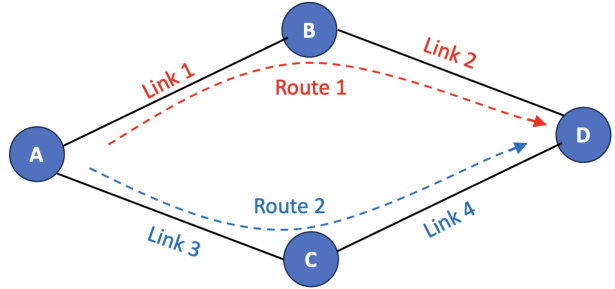


Figure 4. A network is presented with two routing paths from source A to destination D. Path 1 utilizes links 1, 2, while path 2 traverses links 3, 4.

Each link e with has two cores $C = 2$ and each core has $F = 8f_s$. Assume a call requesting $t_i = 4f_s$ arrives and finds the links as shown in **Figure 5a**. Without core switching, the following available continuous and contiguous frequency slots routes are given as follows (**Figure 5b**):

- Route 1 starting frequency slot $f = 5$ using core $c = 2$ on both links. Thus, $\vec{R}_{1,4,5,2,2} = R_{1,4,5,2} + R_{2,4,5,2}$
- Route 2 starting at frequency slot $f = 1$ using core $c = 1$ on both links. Thus, $\vec{R}_{2,4,1,1,1} = R_{3,4,1,1} + R_{4,4,1,1}$
- Route 2 starting at frequency slot $f = 2$ using $c = 2$ on both links. Thus, $\vec{R}_{2,4,2,2,2} = R_{3,4,2,2} + R_{4,4,2,2}$

With core switching, the following added available continuous and contiguous frequency slots routes are given as follows:

- Route 1 starting at frequency slot $f = 3$ using core $c = 1$ on link 1 and $c = 2$ on link 2. Thus, $\vec{R}_{1,4,3,1} + R_{2,4,3,2}$
- Route 2 starting at frequency slot $f = 5$ using core $c = 1$ on link 3 and core $c = 2$ on link 4. Thus, $\vec{R}_{2,4,5,1,2} = R_{3,4,5,1} + R_{4,4,5,2}$

The link-relative costs (R_{e,t_i,f,c_e}) are derived using the method demonstrated in the previous example. Thereafter, the algorithm selects the route exhibiting the minimal $\vec{R}_{r,t_i,f,c}$ value. However, if the minimum $\vec{R}_{r,t_i,f,c}$ value, when multiplied by the discount factor γ , exceeds the call's worth, the call is rejected.

6. Numerical Results

To validate the algorithm presented by us, we developed a specific discrete event simulation. Our simulation was built around the framework of a National Science Foundation network (NSFNET) comprising 14 nodes and 21

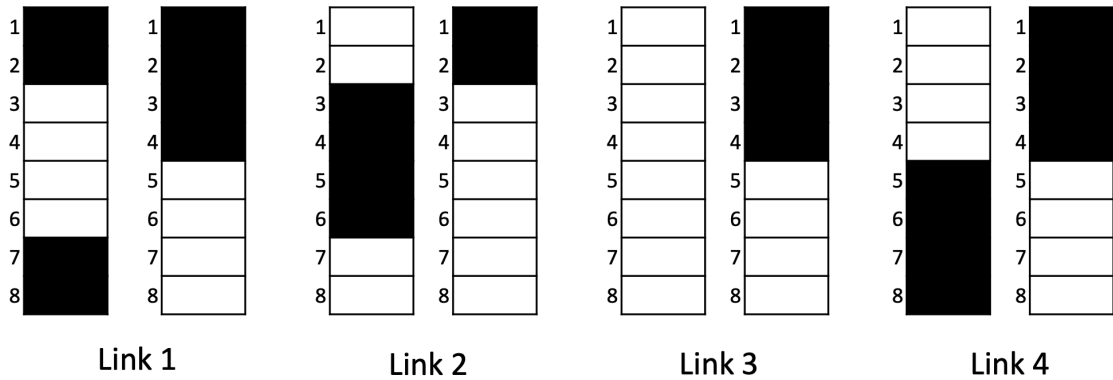


Figure 5. An example of a network with fours links. Each link has two cores $c = 2$ and each core has $f = 8f_s$. An arriving call finds the links in states π_1, π_2, π_3 , and π_4 , with certain frequency slots occupied (colored black) and others unoccupied (colored white). To compute the lost link revenue for links 1, 2, 3, and 4, only the vacant frequency slots are taken into account, while any occupied frequency slots are excluded.

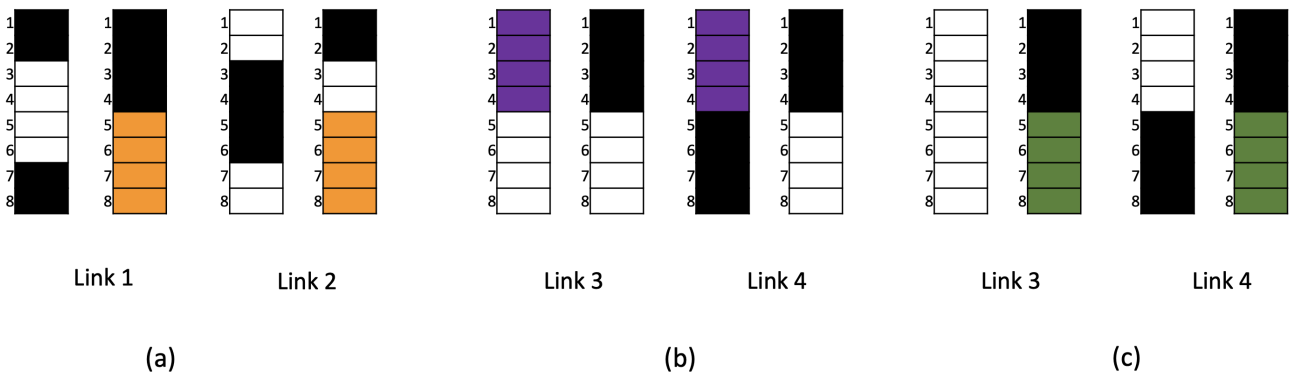


Figure 6. Three continuous and contiguous frequency-slot routes are available without core switching in the illustrated network (see Figure 4 and Figure 5a). The options are as follows: (a) Option one utilizes four frequency slots starting at frequency slot $f = 5$, employing core $c = 2$ on both links 1 and 2. (b) Option two occupies four frequency slots starting at frequency slot $f = 1$, utilizing core $c = 1$ on both links 3 and 4. (c) Option three uses four frequency slots starting at frequency slot $f = 2$, employing core $c = 2$ on both links.

links, as depicted in Figure 7. Within the network, every link is equipped with 7 cores ($C = 7$), and each core's capacity is set at $F = 32f_s$. This network receives four distinct call types ($I = 4$) with a call demand vector denoted as $T = 1, 2, 4, 8$. We considered a uniform distribution of call types, implying that the arrival rate for all call types was identical i.e. $\lambda_1 = \lambda_2 = \lambda_3 = \lambda_4$. The analysis can be extended to incorporate other call arrival distributions, including skewed distributions with high or low skewness, as well as the normal distribution. The same conclusions regarding the performance of the proposed algorithm can be drawn across these different distributions.

A value of $\gamma = 0.5$ is arbitrarily chosen for the discount rate. For a more comprehensive understanding of the significance and impact of the discount rate, we encourage readers to consult the references [8] and [9]. The set of shortest routes was acquired using Dijkstra's algorithm. To ensure statistical validity, we obtained the

average outcome with 95% confidence through twenty-two simulations, each beginning with a distinct random seed. The predefined confidence interval had a width that was less than 1% of the average value.

Interference between cores within the same MCF link is not taken into account. As a result, frequency slots with matching indices can be used in neighboring cores. We examined two different methods for selecting cores: the first one did not involve any classification, referred to as "All common," while the second method included categorization into dedicated and shared cores, known as "Classification." To allocate dedicated cores for call type k in the classification scenario, we employed the normalized demand represented by δ_k and,

$$\delta_k = \frac{t_k \times \lambda_k}{\sum_{i=1}^I t_i \times \lambda_i} \quad (6)$$

The demand for each call type k is calculated by multiplying the arrival rate γ_k by the required number of

slots t_k . With a total of seven cores at our disposal, our assumption was that last three cores would be universally accessible to all calls. The classification of the first four cores are based on $\delta_1 = 7\%$, $\delta_2 = 13\%$, $\delta_3 = 27\%$, and $\delta_4 = 53\%$, (Equation 6). Hence, the first core is assigned to calls type one and two. On the other hand, the second core is dedicated to calls type three while the third and fourth cores are dedicated to calls type four.

Our proposed algorithm will be compared with conventional online routing strategies:

- Fixed Routing (FR): A single pre-defined shortest route is randomly assigned to each call from the available options.
- Fixed Alternate Routing (FAR): FAR employs an exhaustive search method, starting with the shortest route and iteratively evaluating each subsequent path in the predefined sequence until a feasible path is found for the call.
- Least Congested Routing (LCR): The routing algorithm dynamically selects the currently least congested path for each arriving call, this approach utilizes the network's current state to determine the optimal route. Congestion measurement in LCR is premised on the volume of occupied spectrum on a link, signifying that a link with limited available spectrum is considered more congested. While LCR exhibited superior performance compared to FAR in Wavelength Division Multiplexing networks, its performance level in EONs is quite similar.

It's important to emphasize that each of the discussed algorithms includes an admission control mechanism that determines the acceptance or rejection of a call based on the availability of resources. Nevertheless, the admission control of the proposed algorithm integrates fairness. Consequently, the acceptance of a call with lower resource requirements might be refused, even if resources are available, in order to make room for future calls that require more resources.

The first-fit algorithm has been proposed as the most efficient approach for online spectrum allocation in EONs, given that it optimizes spectrum utilization by consolidating utilized spectrum (on one side) to maximize the availability of continuous unused spectrum along a designated route (Christodoulopoulos et al., 2011; Shirazipourazad et al., 2013; Wan et al., 2012). In our numerical tests, we assess both spectrum-then-core and core-then-spectrum first-fit strategies.

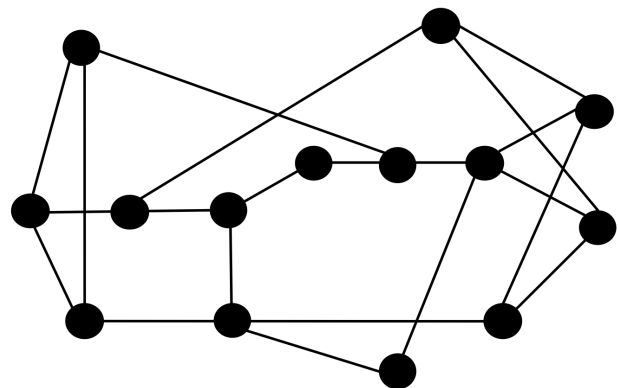
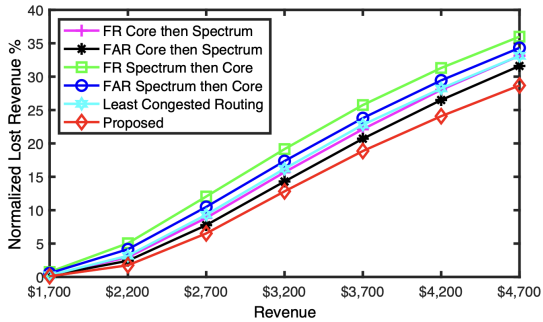


Figure 7. The 14-Nodes NSFNET topology.

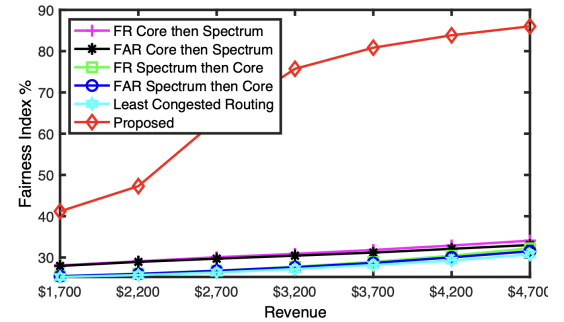
Figures 8 to 10 depict the normalized lost revenue and fairness index across four unique scenarios. These scenarios have been extensively analyzed, taking into account core switching and core classification, while employing different spectrum and routing techniques. The horizontal axis represents the total revenue V , which varies from \$1,700 (under light load) to \$4,700 (under high load). The vertical y-axis depicts either the normalized lost revenue or the fairness index, with both values expressed as percentages.

In the initial scenario illustrated in Figure 8, core classification is absent, resulting in all cores being shared among all call types. Moreover, core switching is permitted. Evidently, the proposed algorithm stands out with the lowest normalized lost revenue. In terms of fairness indices, the algorithm, when combined with admission control, exhibits values ranging from 42% to 86%, whereas other RCSAs show a narrower range of 26% to 32%. To be more specific, the normalized loss revenue undergoes a reduction within the range of 9% to 45%, and the enhancement in fairness varies from 47% to 155%.

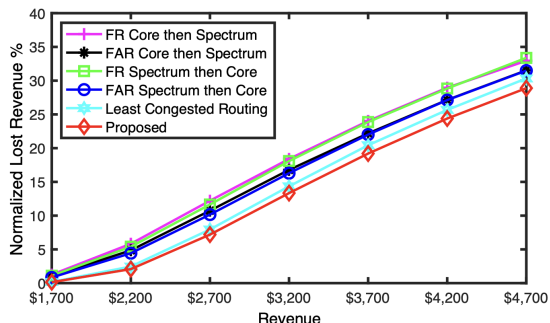
Figure 9 illustrates the second scenario, wherein cores are classified as previously described. In this arrangement, the last three cores universally accessible to all calls. The first core is exclusively allocated to call types one and two, the second core is reserved for call type three, and the third and fourth cores are specifically designated for call type four. Furthermore, the option for core switching is granted. Clearly, the proposed algorithm demonstrates the most minimal normalized lost revenue and the highest fairness index. In this context, the normalized loss revenue experiences a decrease ranging from 5% to 18%, while the improvement in fairness ranges from 10% to 70%.



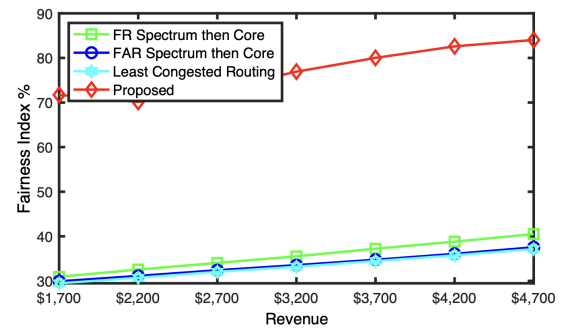
(a) The normalized lost revenue



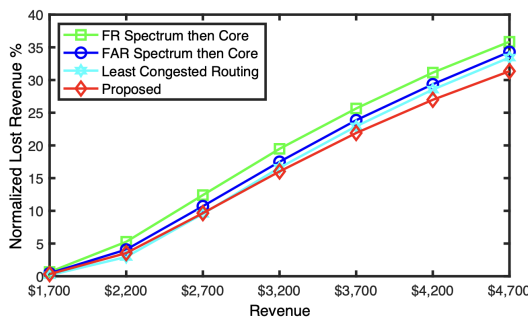
(b) The fairness index

Figure 8. Scenario 1: All cores are common and core switching is permitted.

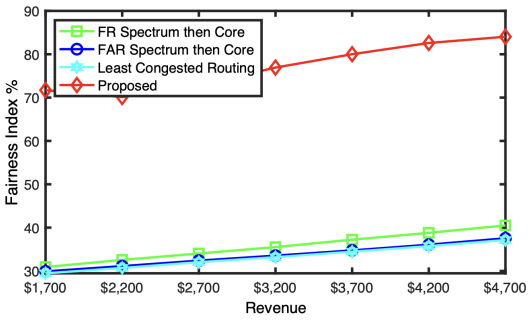
(a) The normalized lost revenue



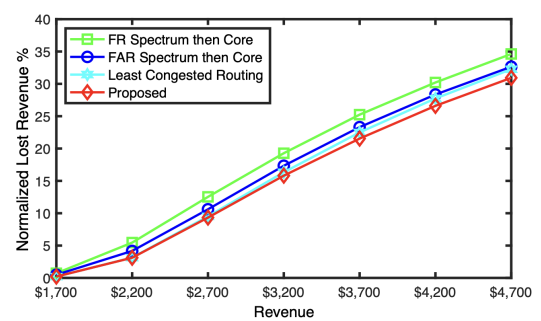
(b) The fairness index

Figure 9. Scenario 2: Cores are classified, and core switching is permitted.

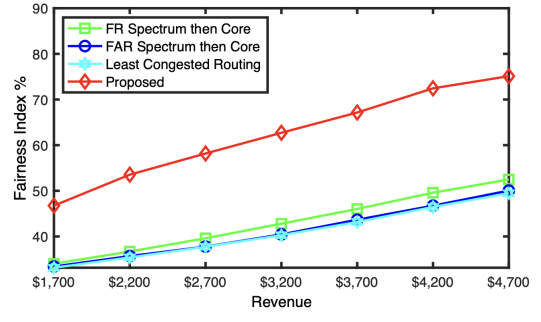
(a) The normalized lost revenue



(b) The fairness index

Figure 10. Scenario 3: All cores are common and core switching is not permitted.

(a) The normalized lost revenue



(b) The fairness index

Figure 11. Scenario 4: All cores are common and core switching is not permitted.

In the third depicted scenario in Figure 10, there is no core classification, which leads to a situation where all cores are shared among all call types. Additionally, core switching is disallowed in this context. The evidence suggests that the proposed algorithm showcases the least amount of normalized lost revenue and the highest values for fairness index. In precise terms, the normalized loss revenue sees a reduction of up to 6%, while the fairness improvement reaches an impressive 132%.

In the last scenario depicted in Figure 11, we apply core classification as outlined in scenario 2. Additionally, core switching is not an option. Among all algorithms tested, the proposed one boasts the lowest normalized lost revenue and the highest fairness index, as measured within this setup. The reduction in normalized lost revenue reaches 4%, accompanied by an increase in fairness of 47%.

7. Conclusion

In our research, we introduced an adaptive algorithm designed for routing, spectrum allocation, and core assignment in networks that employ spatial division multiplexing with multi-core fibers (MCF). This algorithm is enhanced with admission control. The foundation of our proposed algorithm is built upon the concept of relative cost, a notion previously introduced in EON networks. While interference between cores within the same MCF link is not considered in this proposal, it can be readily incorporated in future work without compromising the overall quality of this proposal.

For a new arrival demand, an assessment is conducted across all spectra, core and paths within the pre-computed shortest paths collection. During this process, the relative cost for each link is computed, following which, the cumulative relative cost for the path is determined by summing up the relative costs of its links. The suggested algorithm then opts for the path, spectrum, and core possessing the lowest cumulative relative cost. Regarding admission control, if the relative cost value of a call surpasses its corresponding call worth, the call is declined; otherwise, it is approved.

The numerical results clearly demonstrate the superior performance of the proposed algorithm when compared to other RCSA protocols in terms of network revenue loss and fairness. Additionally, we have provided compelling evidence to underscore the reliability and resilience of the proposed algorithm across various variables, including core classification and core switching. To conclude, our future endeavors will place the emphasis on extending the application of our proposed algorithm to encompass elastic optical networks that incorporate advanced features such as multiple modulation levels, multiple routing options, survivability mechanisms, and RCSA for multicasting scenarios.

References

Alyatama, A. (2014). Fairness in orthogonal frequency-division multiplexing optical networks. *Journal of High Speed Networks*, 20(2):79–93. DOI: 10.3233/jhs-140489.

Alyatama, A. (2016). Computing the single-link performance measurement for elastic optical OFDM. *Photonic Network Communications*, 33(2):125–135. DOI: 10.1007/s11107-016-0624-5.

Alyatama, A. (2017). Analyzing the relative cost concept in elastic optical networks. In *2017 International Conference on Computing, Networking and Communications (ICNC)*, page 886–890. IEEE. DOI: 10.1109/iccnc.2017.7876249.

Alyatama, A. (2020a). Multi-path routing based on relative cost in elastic optical networks. In *2020 7th International Conference on Electrical and Electronics Engineering (ICEEE)*, page 226–231. IEEE. DOI: 10.1109/iceee49618.2020.9102529.

Alyatama, A. (2020b). Relative cost routing and spectrum allocation in elastic optical networks. *Journal of Optical Communications and Networking*, 12(3):38. DOI: 10.1364/jocn.379585.

Alyatama, A. (2021a). Calculating the single-link performance for space division multiplexing elastic optical network. In *2021 8th International Conference on Electrical and Electronics Engineering (ICEEE)*, page 277–282. IEEE. DOI: 10.1109/iceee52452.2021.9415928.

Alyatama, A. (2021b). Relative cost routing, modulation and spectrum allocation in elastic optical networks. In *2021 International Conference on Information Networking (ICOIN)*, page 127–131. IEEE. DOI: 10.1109/icoi50884.2021.9333874.

Christodoulopoulos, K., Tomkos, I., and Varvarigos, E. A. (2011). Elastic bandwidth allocation in flexible OFDM-based optical networks. *Journal of Lightwave Technology*, 29(9):1354–1366. DOI: 10.1109/jlt.2011.2125777.

Da S. Oliveira, H. M. N. and Da Fonseca, N. L. S. (2022). Backup, routing, modulation, spectrum and core allocation in SDM-EON for efficient spectrum utilization. In *2022 IEEE Latin-American Conference on Communications (LATINCOM)*, page 1–6. IEEE. DOI: 10.1109/latincom56090.2022.10000434.

Dlamini, N. N. (2023). Teletraffic engineering/blocking. https://en.wikiversity.org/wiki/Teletraffic_engineering/Blocking. Accessed: 2023-12-19.

Hayashi, T., Taru, T., Shimakawa, O., Sasaki, T., and Sasaoka, E. (2011). Design and fabrication of ultra-low crosstalk and low-loss multi-core fiber. *Optics Express*, 19(17):16576. DOI: 10.1364/oe.19.016576.

Heera, B. S., Sharma, A., Lohani, V., and Singh, Y. N. (2023). Fragmentation-aware rcsa algorithm for fair spectrum allocation in SDM-EON. In *2023 2nd Edition of IEEE Delhi Section Flagship Conference (DELCON)*, page 1–6. IEEE. DOI: 10.1109/delcon57910.2023.10127427.

Lan, Q., Cai, Y., Chen, S., Chen, X., and Shen, J. (2022). A fragmentation-aware load-balanced RM-SCA algorithm in space-division multiplexing elastic optical networks. In *2022 3rd Information Communication Technologies Conference (ICTC)*, page 56–60. IEEE. DOI: 10.1109/ictc55111.2022.9778371.

Lea, C.-T. and Alyatama, A. (1995). Bandwidth quantization and states reduction in the broadband isdn. *IEEE/ACM Transactions on Networking*, 3(3):352–360. DOI: 10.1109/90.392394.

Petale, S. and Subramaniam, S. (2023). Advanced resource allocation strategies for MCF-based SDM-EONs: Crosstalk aware and machine learning assisted algorithms. In *2023 23rd International Conference on Transparent Optical Networks (ICTON)*, page 1–4. IEEE. DOI: 10.1109/icton59386.2023.10207504.

Seki, Y., Tanigawa, Y., Hirota, Y., and Tode, H. (2022). Core and spectrum allocation to achieve graceful degradation of inter-core crosstalk with generalized hierarchical core prioritization on space-division multiplexing elastic optical networks. *Journal of Optical Communications and Networking*, 15(1):43. DOI: 10.1364/jocn.472418.

Sharma, A., Heera, B. S., Lohani, V., and Singh, Y. N. (2022). Fragmentation-aware routing, core and spectrum assignment in multi-core fiber based SDM-EON. In *2022 Workshop on Recent Advances in Photonics (WRAP)*, page 01–02. IEEE. DOI: 10.1109/wrap54064.2022.9758155.

Shirazipourazad, S., Zhou, C., Derakhshandeh, Z., and Sen, A. (2013). On routing and spectrum allocation in spectrum-sliced optical networks. In *2013 Proceedings IEEE INFOCOM*, page 385–389. IEEE. DOI: 10.1109/infcom.2013.6566800.

Vasundhara, Mandloi, A., and Patel, M. (2023). Fragmentation coefficient (FC) conscious routing, core and spectrum allocation in SDM-EON based on MultiCore fiber. In *2023 2nd International Conference on Paradigm Shifts in Communications Embedded Systems, Machine Learning and Signal Processing (PCEMS)*, page 1–4. IEEE. DOI: 10.1109/pcems58491.2023.10136035.

Wan, X., Hua, N., and Zheng, X. (2012). Dynamic routing and spectrum assignment in spectrum-flexible transparent optical networks. *Journal of Optical Communications and Networking*, 4(8):603. DOI: 10.1364/jocn.4.000603.